

Early Pliocene Hominid Tooth from Galili, Somali Region, Ethiopia

Roberto Macchiarelli¹, Luca Bondioli², Dean Falk³, Peter Faupl⁴, Bernard Illerhaus⁵, Ottmar Kullmer⁶, Wolfram Richter⁴, Hasen Said⁷, Oliver Sandrock⁸, Katrin Schäfer⁹, Christoph Urbanek⁴, Bence T. Viola⁹, Gerhard W. Weber⁹ and Horst Seidler⁹

¹ Laboratoire de Géobiologie, Biochronologie et Paléontologie Humaine, CNRS UMR 6046, Université de Poitiers, France

² Sezione di Antropologia, Museo Nazionale Preistorico Etnografico «L. Pigorini», Roma, Italy

³ Department of Anthropology, State University New York, Albany, USA

⁴ Department of Geological Sciences, University of Vienna, Austria

⁵ Federal Institute of Materials Research and Testing (BAM), Berlin, Germany.

⁶ Research Institute Senckenberg, Department of Palaeoanthropology, Frankfurt am Main, Germany

⁷ National Museum of Ethiopia, Addis Ababa, Ethiopia

⁸ Department of Geology, Paleontology and Mineralogy, Hessisches Landesmuseum, Darmstadt, Germany

⁹ Institute of Anthropology, University of Vienna, Austria

ABSTRACT

A fossil hominid tooth was discovered during survey at Galili, Somali region, Ethiopia. The geological and faunal context indicate an Early Pliocene age. The specimen (GLL 33) consists of an almost complete lower right third molar likely representing a male individual of advanced age-at-death. Its comparative metrical, morphological and (micro)structural analysis (supported by a microtomographic record) suggests a tentative taxonomic allocation to Australopithecus cf. A. afarensis.

Key words: lower molar, Australopithecus, Early Pliocene, Galili, Ethiopia

Introduction

The hominid tooth reported here comes from field research activity developed since late 1999 in the Somali Region of Ethiopia by the international Paleo-

Anthropological Research Team (PAR-Team) led by the Institute of Anthropology at the University of Vienna in collaboration with the National Museum of

Ethiopia and the Mekelle University in Ethiopia.

The PAR-Team working area is located on the south-eastern side of the Middle Awash region, in the Afar depression, NE of the recently active northernmost segment of the Main Ethiopian Rift known as the Hertale Graben¹, about 9 km E of the Gedamaitu village (Figure 1). The area, which approximates 100 km², includes two main Neogene vertebrate fossiliferous sub-areas named after their most dominating landscape structures: the Satkawhini (SKW) hill, to NE, and the Galili (GLL) table-top mountain, to SW.

On the first systematic exploratory field survey of the area (on February 2000), the isolated specimen was collected (by Mr. Abdelahi Idle) in recent alluvial debris at the GLL-1/A67 site (9° 77' N, 40° 54' E), located in a depression at about 1 km to the SW of Mount Galili².

The Geochronological and Paleontological Context

The succession of sediments and volcanic rocks exposed nearby Galili belongs to the tectonically elevated eastern rift shoulder of the Main Ethiopian Rift segment. The whole region suffered intensive brittle tectonic deformation, mostly by NNE-SSW-trending faults. Depending on lateral facies variations, the sedimentary sequence is about 120–150 m thick and belongs to the Plio-Pleistocene (4.5–1.6 Ma) »Upper Stratoid Series«³.

Seven main volcanic horizons, comprising basalts, ignimbrites and other pyroclastic layers, have been used as marker beds for subdividing the formation. Based on biostratigraphic record, especially on suids and elephants, the Early to Middle Pliocene sediments represent a relatively short accumulation time span⁴.

Two different successions, separated by a steep, nearly N-S-trending normal fault, exist in the near vicinity of the »hominid site«. In the footwall west of the fault, a morphological scarp exposes about 15 m flat lying sediments, which are composed mainly of grey silty mudstones with thin sand intercalations. In the middle part of the sequence, a conspicuous white limestone bed of 20 cm thickness occurs. Immediately below and above this limestone, further smaller limestone intercalations, sometimes of cellular character, can be observed. The sedimentary succession is overlain by an about 5 m thick ignimbrite, which forms an excellent stratigraphic marker horizon distributed in the entire area. The limestone bed and the accompanying fine clastic sediments represent an ancient shallow lacustrine environment. In the upper part of the section, below the ignimbrite horizon, an increasing fluvial influence can be recognized. In the same stratigraphic niveau, about 2 km towards N, fluvial channels appear (Figure 1).

In the hanging wall east of the fault, a basalt layer, tectonically adjoining the fault, represents the top of the other sedimentary succession, which dips with c. 5° to W. Towards the south of the depression, the basalt forms a morphological ridge. The sediments underlying the basalts mainly comprise poorly sorted, gravely to coarse-grained sands from which, among other fossil remains, primate teeth have been collected. On the basis of grain size analyses, the sandy sediments represent a fluvial facies with high amounts of shelled flood layers. Within the sands, a pyroclastic layer is intercalated about 3.5 m below the basalt.

The eastern succession with the basalt on top is stratigraphically younger than the sediment capped by the ignimbrite towards the west of the fault, well known from regional mapping. The basalt can be correlated with the basalts on top of Mount

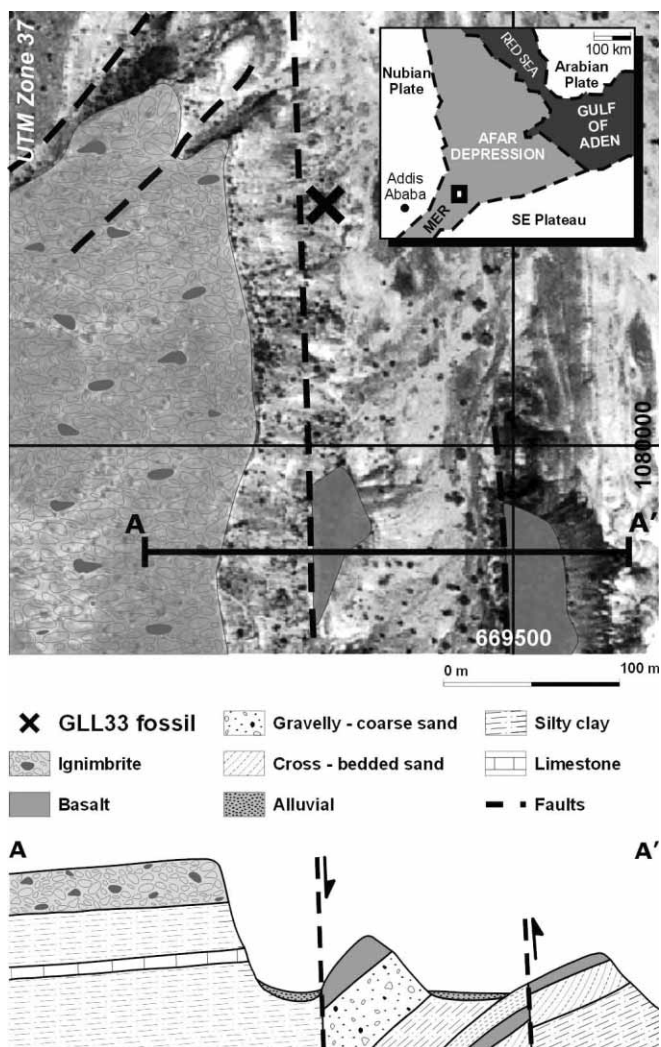


Fig. 1. Schematic placement map of the study region (Somali region of Ethiopia, Afar depression) and stratigraphic diagram of the investigated Mount Galili (GLL) area.

Galili. Radiometric dating ($^{40}\text{Ar}/^{39}\text{Ar}$) of sanidine crystals gained from the ignimbrite gave a preliminary age of 4.1 Ma, which seems in accordance with the biostratigraphic observations (Early Pliocene). Unfortunately, high amounts of excess argon in the basalt lead to analytical problems and unreliable Ar-Ar ages.

From only morphological considerations, both successions, to the W and to the E of the fault, could be the source of the debris containing the hominid tooth. Nonetheless, when taking into account the facies types, the coarse sandy deposits below the basalt layer, which are very rich in faunal remains, should be pre-

ferred to the succession below the ignimbrite which is, in contrast, relatively poor.

The Early Pliocene vertebrate fauna from Galili includes large mammals (Equidae, Rhinocerotidae, Dinotheriidae, Elephantidae, Bovidae, Suidae, Hippopotamidae, Giraffidae, Carnivora, Cercopithecidae), reptiles (Crocodylia, Chelonia), and various species of fish^{2,4}.

Two previous surveys carried out in the region resulted in the discovery of three hominid teeth likely coming from a comparable geochronological context⁵.

The Hominid Tooth (GLL 33): Morphological and Structural Analysis

The hominid specimen from Galili, which is labeled GLL 33, is stored at the National Museum of Ethiopia, Addis Ababa. It consists of a lower right third molar (RM₃) preserving a virtually complete crown but lacking most of the mesial root (Figure 2: A-C). The occlusal surface margins are slightly smoothed and

the appearance of the specimen as a whole (enamel and cementum) testifies to diffuse surface erosion, weathering and local flaking. On the distobuccal aspect, just below the cement-enamel junction (CEJ), a spot-like breakage is present. The distal root, which is nearly complete, shows thin longitudinal and transversal microfractures. Microscopic investigation of the fracture margins of the mesial root evidences erosion at the outer edges, thus suggesting a breakage *in antiquo*.

The general morphology and preservation conditions of GLL 33 are illustrated in Figure 3 (A-I); its overall crown and root metrics are detailed in Table 1.

The occlusal outline is a rectangle tapering distally to form a convex margin. The crown bears seven cusps, including a developed *tuberculum intermedium* (metaconulid) occurring in the lingual groove between metaconid and entoconid. Relative cusp sizes (decreasing order) are protoconid (c1), metaconid (c2), hypoconid (c3), hypoconulid (c5), entoconid (c4), metaconulid (c7), entoconulid (*tuberculum sextum*, c6).

According to the ASU coding system for nonmetric dental traits⁶, cusp 5 and cusp 7 (both degree 4) are proportionally large, while cusp 6 (degree 2) is slightly smaller than cusp 5. The occlusal fissural pattern is Y7, with metaconid-hypoconid contact. On the distobuccal aspect, a ^-shaped fissure is detectable between c3 and c5; a deep distolingual groove separates c4 and c7. Secondary fissures run towards the central basin. Because of occlusal surface weathering at the metaconid distal side, deflecting wrinkle occurrence cannot be properly assessed. A smooth, faintly developed mesial trigonid crest connects protoconid and metaconid; the distolingual groove is distinct. Metaconid and hypoconulid are rather mesially and buccally placed, respectively; the entoconulid is double. The anterior fovea (precuspidal fossa) is present (degree 2),

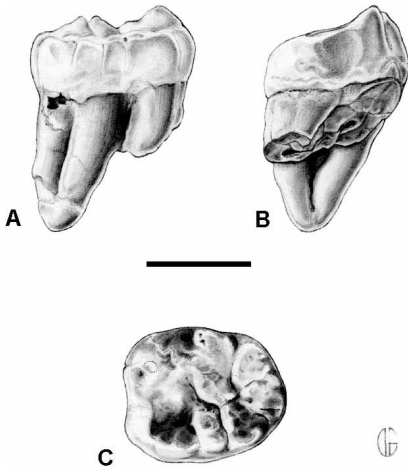


Fig. 2. Drawing of GLL 33 in buccal (A), mesial (B), and occlusal (C) views (courtesy of Heidemarie Grillitsch, Inst. of Zoology, University of Vienna). Bar is 1 cm.

while the posterior one is absent; the paracristid is mesially placed. On the buccal crown side, just below c1, a hardly traceable protostylid appears as a faint buccal fissure curved to distal (degree 2).

Notably in distal view, a relative retention of the occlusally projecting edges of the lingual cusps is evident, while the buccal cusps are almost flat (rather ho-

mogeneous linguobuccal wear gradient towards flattening). Metaconid and protoconid are the most salient and the most worn cusps, respectively, the latter showing a single occlusal emerging dentine pinpoint spot on its buccal slope (the only GLL 33 enamel perforation). Relative cusp wear (decreasing order) is c1, c3, c5, c6, c2, c7, c4. While the distal crown mar-

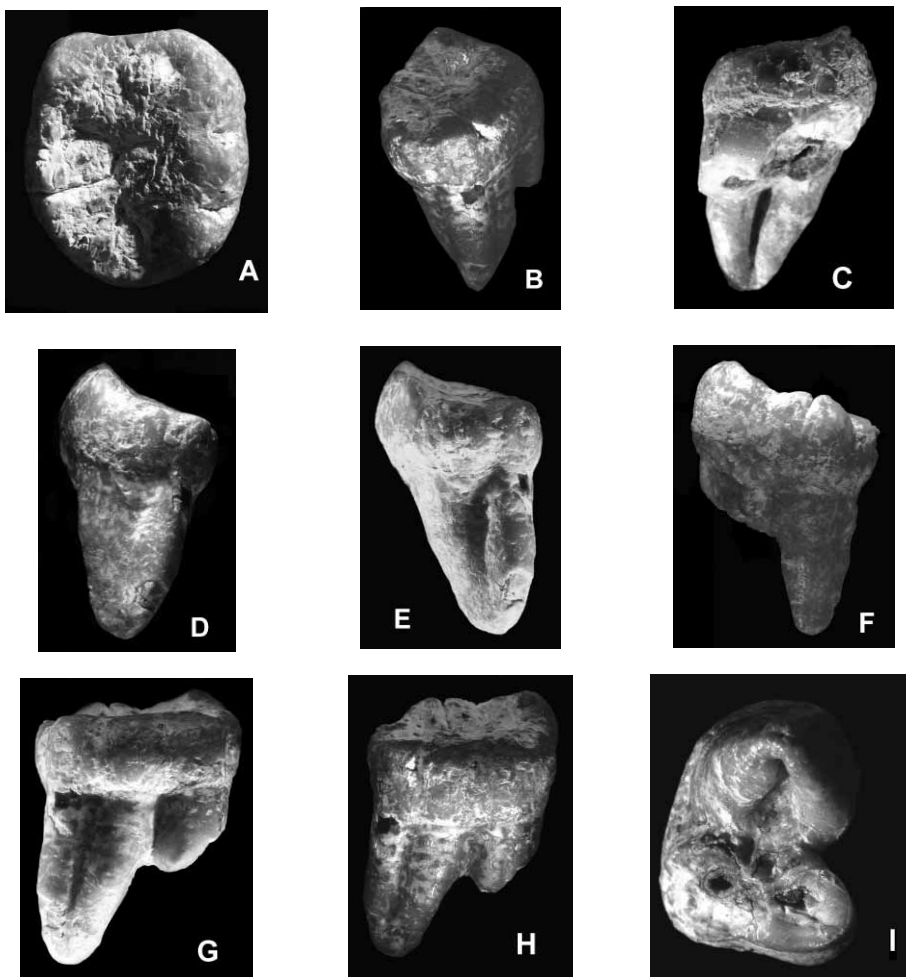


Fig. 3. GLL 33 general morphology and preservation. A: occlusal aspect; B: oblique distobuccal view; C: mesial aspect; D: distal aspect; E: slightly oblique distal view; F: lingual aspect; G: buccal aspect; H: slightly oblique buccal view; I: apical view. Images not to scale.

TABLE 1
 GLL 33 CROWN AND ROOT METRICS. LINEAR MEASUREMENTS IN MM; AREAS IN MM²

Variable	Value
1 Occlusal mesiodistal diameter (distance between the mesial and the distal edges)	15.6
2 Maximum occlusal mesiodistal diameter (estimated max. distance between the mesial and the distal edges avoiding the interproximal mesial wear)	16.3
3 Maximum mesiodistal diameter (max. distance between the mesial and the distal surfaces)	16.6
4 Maximum buccolingual diameter (max. distance between the buccal and the lingual surfaces)	14.3
5 Occlusal buccolingual diameter at mid-crown	13.9
6 Maximum buccolingual diameter across protoconid	14.2
7 Maximum buccolingual diameter across hypoconid	14.3
8 Maximum crown height at metaconid (projecting distance between CEJ at the mesiolingual aspect and the metaconid apex)	7.5
9 Maximum crown height at entoconid (projecting distance between CEJ at the distolingual aspect and the entoconid apex)	6.8
10 Minimum occlusal surface area (var. 1 x var. 5)	216.8
11 Maximum occlusal surface area (var. 2 x var. 5)	226.6
12 Crown area (var. 2 x var. 4)	233.1
13 Maximum cross-sectional crown area (var. 3 x var. 4)	237.4
14 Crown shape (var. 2 / var. 4)	1.14
15 Maximum height of the distal root (along the distal aspect)	14.1
16 Mesiodistal diameter of the distal root at furcation	8.0

gin around hypoconulid and entoconulid is rounded, a large, from flat to sub-concave, oval-shaped interproximal wear facet involving both protoconid and metaconid is present on the mesial tooth aspect, with a buccolingually oriented major axis (height: 4.4 mm; width: 6.5 mm).

Even at a low magnification (6x hand lens), perikymata are detectable on the crown's buccal aspect, notably at the level of the hypoconulid. Perikymata density increases towards the cervical margin, where they show a sinusoidal path. Moving along a linear distance of 5 mm from the CEJ towards the c5 apex (even if not really up to its tip), a total of 39 perikymata has been recorded.

Despite weathering which may have locally masked, or even erased, some enamel surface (micro)features, no evidence for linear enamel hypoplasia, hypocalcifications or enamel macro-defects is found on GLL 33, and no crenulated appearance of the enamel is seen in occlusal view.

GLL 33's radiographic and high resolution x-ray computed microtomographic record (see *infra*) show that the broken mesial root has two canals filled by fine sediment. The complete distal root is well grooved and flattened mesiodistally. It is rather inclined with respect to the horizontal plane but not bent, and shows full apical closure with a single canal. The ce-

mentum, which is well preserved on this root despite some buccal chippings, is rather thick.

In order to investigate its inner morphology and to detail its enamel thickness topographic variation, GLL 33 was scanned by means of a μ CT-scan system at the Bundesanstalt fuer Materialforschung und-pruefung (BAM), Berlin. Microtomographic analysis was made with the exposure of 0.2 mA at 110 kV for 14.000 msec with a 2 mm copper prefilter. The radiographic images were collected by a 1024 by 1024 pixel CCD camera coupled with an image intensifier. Following a 360° rotation of the specimen, 720 images (each at 0.5°) were taken with a pixel resolution of 0.033027 mm. For volume rendering and imaging, two data sets at 30 μ and 60 μ voxel resolution were primarily reconstructed from the raw microtomographic data by means of AVS 5.3 (Advanced Visual Systems, Inc.) and AMIRA 3.1 (TGS Inc.), resulting in a volume of 899 x 899 x 553 and 450 x 450 x 277 matrix size, respectively. A μ CT-based three-dimensional reconstruction of the fossil hominid tooth from Galili is shown in Figure 4.

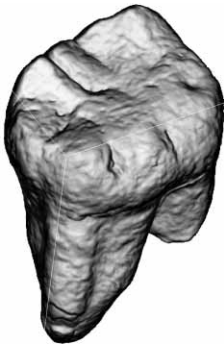


Fig. 4. μ CT-based three-dimensional reconstruction of GLL 33 (oblique distobuccal view).

To allow independent elaboration and analysis of this high-resolution μ CT re-



Fig. 5. GLL 33. Lingual view of the μ CT mesiodistal section through the mid-crown showing the filled pulp chamber.

cord, likely the first one realized on a Early Pliocene hominid tooth, we have made the original digitized volume data fully available at <http://www.anthropology.at/virtanth/webshop.php>.

Likely following the partial breaking of the mesial root, the pulp chamber has been entirely filled by fine sediment particles (Figure 5). The μ CT-based three-dimensional rendering (transparency) of the pulp chamber and the radicular canal(s) is shown in Figure 6. The maximum width of the pulp chamber (measured over the floor to furcation) is 7.6 mm; the total volume (chamber and distal radicular canal) is 103.2 mm³.

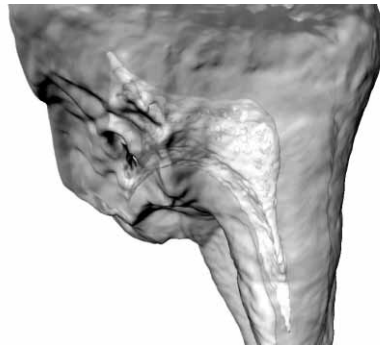


Fig. 6. GLL 33. Lingual view of the μ CT-based three-dimensional rendering (transparency) of the pulp chamber and root canal(s).

Pulp chamber volume variation in early hominid molars is still unknown. Nonetheless, based on extant human figures, the rather low position in GLL 33 of its ceiling with respect to the occlusal plane (ceiling found at the CEJ level in 97% of extant human lower molars⁷), its modest width in both mesiodistal and buccolingual directions, and a certain degree of resorption observed around the lower portion of the distal canal would suggest an adult-mature age-at-death for this individual.

While the enamel is worn and weathered at the surface, its inner structure is only very modestly affected by the multidirectional micro-cracks and fractures involving both dentine and cementum (Figure 7).



Fig. 7. GLL 33. Lingual view of the μ CT mesiodistal section taken midway between the mid-crown and the buccal aspect showing multidirectional micro-cracks/fractures mostly affecting dentine and cementum.

Before GLL 33 was μ CT-scanned, linear enamel thickness had been preliminarily measured by a digital caliper directly at the level of the mesiolingual margin of the dentine spot emerging on the lingual slope of the protoconid (0.75 mm). Based on the currently available high-resolution microtomographic record,

a number of standardized measurements have been realized through: (1) the metaconid-protoconid (m-p) mesial section (five measures), (2) the entoconid-hypoconid (e-h) distal section (four measures), (3) the metaconid-entoconid (m-e) lingual section (nine measures), and (4) the protoconid-hypoconid (p-h) buccal section (two measures). With specific reference to the GLL 33 lingual section through metaconid and entoconid, Figure 8 schematizes the site of nine key-points set along the enamel-dentine junction (EDJ) and the related linear enamel thickness measures tentatively performed on the four investigated sections (for a discussion concerning the different methodological approaches used in assessing enamel thickness in extant and extinct primates, see^{8–13}).

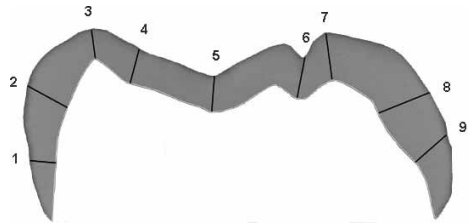


Fig. 8. Topographic distribution of the nine standard points set along the enamel-dentine junction (EDJ) and indication of the enamel thickness (ET) measurements taken in the present study. The GLL 33 μ CT lingual section through metaconid (left) and entoconid (right) cusps is used as reference scheme for all the four investigated sections (m-p, e-h, m-e, and p-h). ET measure 1: taken at 1/3 of the EDJ length between cervix and dentin horn (here, on the mesial side); 2: as measure 1 but at 2/3; 3: between the dentine horn and the cusp apex (here, the metaconid); 4: at 1/6 of the EDJ length between the two dentine horns; 5: from the inferiormost intercusp point along the EDJ to the analogous point on the outer enamel; 6: as measure 4 but at 5/6; 7: as 3 (here, the entoconid); 8: as measure 2 (here, on the distal side); 9: as measure 1 (here, on the distal side).

TABLE 2
GLL 33 μ CT-BASED ENAMEL THICKNESS (ET)
TOPOGRAPHIC VARIATION

ET measure	m-p	e-h	m-e	p-h
1	0.72	1.01	0.92	0.5
2	1.72	1.67	1.52	–
3	1.34	2.03	1.07	–
4	–	–	1.29	–
5	1.39	–	1.29	–
6	–	–	2.09	–
7	–	–	1.69	–
8	–	–	1.93	–
9	0.84	0.97	1.33	1.44

m-p: metaconid-protoconid (mesial) section; e-h: entoconid-hypoconid (distal) section; m-e: metaconid-entoconid (lingual) section; p-h: protoconid-hypoconid (buccal) section. For the description of the 1-9 ET variables, see Figure 7. Values in mm.

The set of 20 (on 36 possible) μ CT-based measures actually taken on GLL 33 (by means of the MPSPK original software) are shown in Table 2. Because of the distinct linguobuccal wear gradient, as well as of the mild but diffuse erosion

affecting enamel, all values are doubtless underestimated, with the only likely exception of those measured along the metaconid-entoconid (lingual) section. It should be also noted that, by definition, a mesiodistally- and a buccolingually-oriented section systematically intersects at the cuspal level (m-p and p-h at c1; m-p and m-e at c2; e-h and p-h at c3; e-h and m-e at c4).

As expected because of occlusal crown topography, the highest individual and average thickness values are found along the m-e lingual section (2.09 mm close to the entoconid and 1.5 mm, respectively), while the minimal ones concern the protoconid-hypoconid buccal section (0.50 mm and 1.0 mm, respectively). Mostly because of the value recorded at the entoconid apex (2.03 mm), the average thickness shown by the entoconid-hypoconid distal section (1.4 mm) approximates the m-e figures.

In a methodological perspective, it is worthwhile to note that, while corresponding to the metaconid and to the

TABLE 3
LOWER M3 COMPARATIVE TOOTH METRICS. LINEAR MEASUREMENTS IN MM; AREAS IN MM²

Taxon/sample/specimen	Mesiodistal					Buccolingual				
	N	X	SD	Min.	Max	N	X	SD	Min.	Max
GLL 33	1	16.3 ^a				1	14.3 ^b			
<i>A. anamensis</i> : Kanapoi ³⁰	6	14.6	1.19	13.7	17.0	6	12.8	0.66	11.9	13.4
Allia Bay ³⁰	1	15.7				1	13.7			
<i>A. afarensis</i> ³⁰	22	15.1	1.18	13.4	17.4	19	13.4	0.99	11.3	15.3
Maka ²⁹	4			14.8	16.2	4			13.0	13.8

Taxon/sample/specimen	Crown area (MD x BL)					Crown shape (MD/BL)				
	N	X	SD	Min.	Max	N	X	SD	Min.	Max
GLL 33	1	233.1 ^c				1	1.14 ^d			
<i>A. anamensis</i> : Kanapoi ³⁰	7	182.1	26.6	153.2	227.8	7	1.10	0.15	0.80	1.27
Allia Bay ³⁰	1	215.1				1	1.15			
<i>A. afarensis</i> ³⁰	18	199.0	27.0	151.4	266.2	18	1.13	0.06	0.99	1.21
Maka ²⁹	4			192.4	223.6	4			0.85	0.88

^a var. 2 in Table 1; ^b var. 4 in Table 1

^c var. 12 in Table 1; ^d var. 14 in Table 1

entoconid cusps, respectively, the thickness values recorded for the pairs m-p3 (1.34 mm) / m-e3 (1.07 mm) and e-h3 (2.03 mm) / m-e7 (1.69 mm) differ because of their different sectional orientation.

Even if quantitatively limited and qualitatively affected by functional and taphonomic histories, the GLL 33 record confirms the highly site-specific nature of enamel thickness variation in hominid molars^{10,11}. Growing evidence shows that hominid enamel thickness varies by location within the crown, along serial position, and between individuals of a taxon¹⁴. This points to the need for the systematic application of advanced non-invasive investigative methods capable of minimizing the risk of inconsistent assessments^{15,16}.

A method to quantify and to compare overall enamel thickness of a molar by means of an average thickness value has been elaborated by Martin^{8,17} by sectioning the crown through the mesial cusps and by dividing the cross-section of enamel by the EDJ length. In the case of GLL 33, because of the linguobuccal wear gradient and related functional enamel loss, the index has been assessed with reference to the metaconid-entoconid (m-e) lingual section. The (adimensional) value obtained (19.1), which is lower than the figures currently available for *Australopithecus africanus* (21.4), *Homo sapiens* (22.4), *Paranthropus robustus* (29.6), and *P. boisei* (34.9)¹⁸, falls in the category »thick enamel«¹⁷.

Comparisons and Tentative Taxonomic Assessment

Hominid (lower) M3s are highly variable and thus of low potential value for reliable taxonomic assessment. Nonetheless, taking also into account its likely chronological position (Early Pliocene), some critical remarks based on the comparative analysis of the currently avail-

able hominid dental record are possible for the GLL 33 specimen.

General external size, morphology and the enamel thickness of the RM₃ from Galili clearly differ from the primitive conditions reported for Early Pliocene *Ardipithecus ramidus*¹⁹ and completely resemble the conditions reported for the taxon *Australopithecus*^{20–30}. Notably, GLL 33 crown metrics/proportions, likely indicating a male individual, fall within the range of variation shown by *A. anamensis* and *A. afarensis* (Table 3).

External crown dimensions of *A. anamensis* teeth are generally comparable to those of *A. afarensis* (the greatest difference being the larger lower I2 observed in *A. anamensis*³⁰). These taxa also share a similar occlusal molar topography^{23,24,29,30}, with the protoconid (as in GLL 33) or metaconid the largest cusps on lower molars. Even the wear pattern is similar, with a strong buccal/lingual discrepancy^{29,30} (the same observed on GLL 33). Conversely, compared to the *A. afarensis* condition, and to GLL 33 as well, the *A. anamensis* lower molars (e.g., KNM-KP 30500) are lower-crowned and have much more sloping buccal sides, while the lingual surface is steep^{26,27,30}. Another possible difference among the two taxa concerns the occurrence and degree of expression of cingular remnant features, such as the protostylid on the lower molars, which are more common and more expressed in *A. anamensis* than in *A. afarensis*, where they appear in form of pits/mild ridges^{22,25,30} (as in GLL 33). On the other hand, hominin specimens from Kataboi and lower Lomekwi Members attributed to *Kenyanthropus platyops* exhibit a suite of features that distinguishes them from other hominin taxa. According to Leakey and co-workers³¹, while its enamel thickness (as measured in specimens such as KNM-WT 38350 and WT 40000) is comparable to that in *A. anamensis* and *A. afarensis*^{27,31}, *K. pla-*

tyops differs from *A. anamensis*, *A. afarensis*, *A. africanus*, and *A. garhi* in having small (upper) molars.

As regards to enamel thickness, *A. anamensis* linear measurements indicate relatively thick enamel (the thickness near cusp apices can be measured between 1.5 and 2.0 mm²⁷), but less than reported for robust australopithecines¹⁰. In KNM-ER 30749 *A. anamensis* lower M1³⁰, the buccolingual section through hypoconid displays values which overlap those from GLL 33 (buccal occlusal basin = 1.6 mm; buccal cusp tip = 1.0 mm; buccal cervical wall = 1.8 mm). Also, naturally cracked *A. anamensis* molars have enamel as thick as that reported for *A. afarensis*²⁷ (for comparative measures on an *A. afarensis* lower P4, see²⁹).

In conclusion, several elements support a generic attribution of the RM₃ from Early Pliocene Galili to the taxon *Australopithecus*. Interestingly, preliminary analyses of three hominid teeth previously discovered in the same region suggest they may belong to a species »more primitive than *Australopithecus afarensis* and more like *Australopithecus anamensis*«⁵. Nonetheless, notably because of its comparatively high crown (see var. 8 and 9 in Table 1) and of the outline of its lingual aspect, the best tentative allocation for GLL 33 is to *Australopithecus* cf. *A. afarensis* (being specimens such as A.L. 266-1 and 400-1a from Hadar, MAK-

VP-1/2 and 1/12 from Maka, and L.H. 4 from Laetoli the closest match for general crown size and occlusal shape). Only a detailed comparison among the specimens collected to date at Galili and, mostly, additional recoveries in the area will elucidate the possible relationships between *A. anamensis* and *A. afarensis*.

Acknowledgements

Since late 1999, the research activities promoted by the PAR-Team have received the constant support of the Ethiopian Ministry of Culture and Information. The 2000 field survey in the Satkawahini and Galili areas was specifically supported by the Austrian Federal Ministry for Education, Science and Culture (Project No. BM:BWK 200.049/3–VI/1/387/25-30) and the Austrian Council for Science and Technology, the Italian National Research Council (PF »Beni Culturali«), and the Italian Ministry of Cultural Heritage (to LB and RM). Special thanks for their collaboration are due to Ato Jara Haile Mariam (ARCCH Addis Ababa), H.E. Woldemichael Chamo (Ethiopian Minister for Cultural Affairs and Information). For their scientific contribution to the project, we are also indebted to G.C. Conroy, H. Prossinger, D.S. Weaver. GLL 33 drawings (Figure 2) and pictures (Figure 3) courtesy of H. Grillitsch, and R. Ginner, respectively.

REFERENCES

1. CHRISTIANSEN, T. B., H.-U. SCHAEFER, M. SCHÖNFELD, Southern Afar and adjacent areas: Geology, petrology, geochemistry. In: PILGER, A., A. RÖSLER (Eds.): Afar depression of Ethiopia. (Schweizerbart, Stuttgart, 1975). — 2. WEBER, G. W., H. SEIDLER, R. MACCHIARELLI, L. BONDIOLI, P. FAUPL, W. RICHTER, O. KULLMER, O. SANDROCK, D. FALK, Am. J. Phys. Anthropol., 32 Suppl. (2001) 162. — 3. CHERNET, T., W. K. HART, J. L. ARONSON, R. C. WALTER, J. Volc. Geotherm. Res., 80 (1998) 267. — 4. URBANEK, C., O. KULLMER, O.

SANDROCK, P. FAUPL, D. NAGEL, B. VIOLA, H. SEIDLER, In: Proceedings. (32nd Int. Geol. Congr., Florence, 2004). — 5. HAILE-SELASSIE, Y., B. ASFAW, Am. J. Phys. Anthropol., 30 Suppl. (2000) 170. — 6. TURNER II, C. G., C. R. NICHOL, G. R. SCOTT, Scoring procedures for key morphological traits of the permanent dentition: The Arizona State University Dental Anthropology System. In: KELLEY, M. A., C. S. LARSEN (Eds.): Advances in dental anthropology. (Wiley-Liss, New York, 1991). — 7. DEUTSCH, A. S., B. I. COHEN, B. L. MUSIKANT,

- In: Proceedings. (The IADR/AADR/CADR 82nd General Session, Honolulu, 2004). — 8. MARTIN, L. B.: The relationships of the later Miocene Hominoidea. Ph.D. Thesis. (University College London, London, 1983). — 9. BEYNON, A. D., B. A. WOOD, Am. J. Phys. Anthropol., 70 (1986) 177. — 10. GRINE, F. E., L. B. MARTIN, Enamel thickness and development in *Australopithecus* and *Paranthropus*. In: GRINE, F. E. (Ed.): Evolutionary history of the »robust« Australopithecines. (Aldine de Gruyter, New York, 1988). — 11. MACHO, G. A., M. A. BERNER, Am. J. Phys. Anthropol., 92 (1993) 189. — 12. MACHO, G. A., Arch. Oral Biol., 39 (1994) 783. — 13. SCHWARTZ, G. T., Am. J. Phys. Anthropol., 111 (2000) 221. — 14. SUWA, G., T. D. WHITE, F. C. HOWELL, Am. J. Phys. Anthropol., 101 (1996) 247. — 15. MAZURIER, A., L. BONDIOLI, S. CAROPRESO, R. MACCHIARELLI, Am. J. Phys. Anthropol., 36 Suppl. (2003) 148. — 16. SUWA, G., R. T. KONO, M. BRUNET, T. D. WHITE, In: Proceedings. (Paleoanthrop. Assoc. Meeting, Tempe, 2003). — 17. MARTIN, L. B., Nature, 314 (1985) 260. — 18. SMITH, T. M., L. B. MARTIN, M. G. LEAKEY, J. Hum. Evol., 44 (2003) 283. — 19. WHITE, T. D., G. SUWA, B. ASFAW, Nature, 371 (1994) 306. — 20. WHITE, T. D., Am. J. Phys. Anthropol., 46 (1977) 197. — 21. WHITE, T. D., Am. J. Phys. Anthropol., 53 (1980) 487. — 22. WHITE, T. D., D. C., JOHANSON, W. KIMBEL, S. Afr. J. Sci., 77 (1981) 445. — 23. JOHANSON, D. C., T. D. WHITE, Y. COPPENS, Am. J. Phys. Anthropol., 57 (1982) 545. — 24. WHITE, T. D., D. C. JOHANSON, Am. J. Phys. Anthropol., 57 (1982) 501. — 25. WHITE, T. D., The hominids of Hadar and Laetoli: An element-by-element comparison of the dental samples. In: DELSON, E. (Ed.): Ancestors: The hard evidence. (Alan R. Liss, New York, 1985). — 26. COFFING, K., C. FEIBEL, M. LEAKEY, A. WALKER, Am. J. Phys. Anthropol., 93 (1994) 55. — 27. LEAKEY, M. G., C. S. FEIBEL, I. MCDUGALL, A. WALKER, Nature, 376 (1995) 565. — 28. LOCKWOOD, C. A., W. H. KIMBEL, D. C. JOHANSON, J. Hum. Evol., 39 (2000) 23. — 29. WHITE, T. D., G. SUWA, S. SIMPSON, B. ASFAW, Am. J. Phys. Anthropol., 111 (2000) 45. — 30. WARD, C. V., M. G. LEAKEY, A. WALKER, J. Hum. Evol., 41 (2001) 255. — 31. LEAKEY, M. G., F. SPOOR, F. H. BROWN, P. N. GATHOGO, C. KIARIE, L. N. LEAKEY, I. MCDUGALL, Nature, 410 (2001) 433.

R. Macchiarelli

Lab. de Géobiologie, Biochronologie et Paléontologie Humaine, CNRS UMR 6046, Université de Poitiers, 40 av. du Recteur Pineau, 86022 Poitiers, France
e-mail: Roberto.Macchiarelli@univ-poitiers.fr

ZUB RANOG PLIOCENSKOG HOMINIDA IZ GALILIJE, REGIJA SOMALI, ETIOPIJA

SAŽETAK

Fosilni zub hominida otkriven je tijekom istraživanja u Galiliji, regija Somali, Etiopija. Geološki i faunalni kontekst sugerira vrijeme ranog Pliocena. Uzorak (GLL 33) sastoji se od gotovo kompletnog donjeg desnog trećeg kutnjaka koji najvjerojatnije odgovara muškoj osobi starije dobi. Usporedne metričke, morfološke i (mikro)strukturne analize (poduprte mikrotomografskim zapisom) ukazuju na provizorno taksonomsko određenje kao pripadnika roda *Australopithecus*, vrste cf. *A. afarensis*.